

**SOME CONSIDERATIONS OF AN AXIAL ARC  
IN A RADIAL MAGNETIC FIELD**

---

**A Thesis**

**Presented to**

**The Faculty of the Department of Physics  
The College of William and Mary in Virginia**

---

**In Partial Fulfillment**

**Of the Requirements for the Degree of  
Master of Arts**

---

**By**

**Philip Brockman**

**May 1963**

**APPROVAL SHEET**

This thesis is submitted in partial fulfillment of  
the requirements for the degree of  
Master of Arts

*Philip D. [unclear]*  
Author

Approved, May 1965:

*Donald E. McLennan*  
Donald E. McLennan, Ph.D.

*Frederic E. Crowfield, Jr.*  
Frederic E. Crowfield, Jr., Ph.D.

*James D. Lawrence, Jr.*  
James D. Lawrence, Jr., Ph.D.

---

#### ACKNOWLEDGEMENTS

The author is grateful for the guidance and criticism of Professor D. E. McLennan during the course of this project. The author also wishes to express his appreciation to R. V. Hees, Section Head, Plasma Physics Section, National Aeronautics and Space Administration, Langley Research Center for his many helpful suggestions and discussions during this investigation.

TABLE OF CONTENTS

	Page
ACKNOWLEDGMENTS . . . . .	iii
LIST OF FIGURES . . . . .	v
LIST OF SYMBOLS . . . . .	vi
ABSTRACT . . . . .	vii
INTRODUCTION . . . . .	2
APPARATUS . . . . .	5
DEVELOPMENT OF EQUATIONS . . . . .	8
OPERATION OF DISCHARGE AND MEASUREMENTS . . . . .	12
INTERPRETATION OF RESULTS . . . . .	28
REFERENCES . . . . .	36

## LIST OF FIGURES

Figure	Page
1. Schematic diagram of apparatus . . . . .	9
2. Schematic diagram of magnetic field shape . . . . .	11
3. Plots of Hall current density versus axial current density for various magnetic flux densities . . . . .	15
4. Plots of Hall current density versus magnetic flux density for various axial current densities . . . . .	18
5. Plots of electric field strength versus axial current density for various magnetic flux densities . . . . .	21
6. Plots of electric field strength versus magnetic flux density for various axial current densities . . . . .	24
7. Plot of $1/W$ and $W/(1 + W^2)$ for axial current density of 5240 amperes per square meter at 30 microns Hg . . . . .	32
8. Theoretical and experimental plots of Hall current density versus magnetic flux density at axial current densities of 3930, 5240, and 9170 amperes per square meter at 30 microns Hg . . . . .	33
9. Theoretical and experimental plot of electric field strength versus magnetic flux density at an axial current density of 5240 amperes per square meter at 30 microns Hg . . . . .	34

## LIST OF SYMBOLS

$\vec{H}$	magnetic flux density
$e$	charge on singly ionized ion
$\vec{E}$	electric field strength
$\vec{E}'$	$\vec{E}' = \vec{E} + \vec{v} \times \vec{B}$
$\vec{j}$	current density
$m_e, m_i$	mass of particle
$m$	meter
$n$	particle density
$p$	pressure
$t$	time
$\vec{v}$	center of mass velocity
$W$	$W = (1 + \sum \sum \tau_e \omega_i \tau_i) / \omega_e \tau_e$
$\sigma$	conductivity
$\tau$	mean time between collisions of particle species
$\mu$	microns
$\omega_e, \omega_i$	cyclotron frequency, $\omega_e = eB/m_e, \omega_i = eB/m_i$
Subscripts:	
$e$	electron
$i$	ion
$o$	conditions with no magnetic field
$r, \theta, z$	refers to cylindrical coordinate system
Superscript:	
$(\vec{\quad})$	vector quantity

## ABSTRACT

Ball currents have been measured in the Linear Hall accelerator at pressures from 15 to 40 microns of mercury in argon at currents from 10 to 40 amps at voltages from 100 to 600 volts and at magnetic field strengths from 12.5 to 550 gauss. Ball current at constant axial current shows an increase to a maximum and a subsequent decrease with increasing magnetic field strength. A tentative theory based on the increase of ion slip with increasing magnetic field strength is proposed and agreement with experiment is shown.

**SOME CONSIDERATIONS OF AN AXIAL ARC  
IN A RADIAL MAGNETIC FIELD**

## INTRODUCTION

When a current passes through a magnetic field there is a Lorentz force on the moving charges. This force is, in the case of the electrons,  $-ev\vec{v}\times\vec{B}$ . If a conducting bar is placed perpendicular to a magnetic field and a current is passing through the bar, the Lorentz force on the electrons will result in a potential occurring across the bar in a direction perpendicular to both the magnetic field and the current. This effect is known as the Hall effect and the potential is called the Hall potential. If the bar were to be replaced with a conducting cylinder in a radial magnetic field such that the field is everywhere perpendicular to the cylinder, the Lorentz force would result in a current in the azimuthal direction. This current, which is known as the Hall current, will be perpendicular to both the magnetic field and the original current.

As the Hall current is perpendicular to the magnetic field, a Lorentz force will also act on the electrons in the Hall current and this force will be opposed to the original electron motion. R. V. Hess of Langley Research Center, National Aeronautics and Space Administration, proposed in 1959 to use the Hall current for plasma acceleration (ref. 1). The device investigated at that time consisted of a radial arc in a magnetic field with both axial and radial components. The Hall current was supplied by the radial current and axial field component. The accelerating force was supplied by the Hall current and

radial field. The ions were accelerated through space charge interaction with the electrons.

More recently a device has been proposed (ref. 2) which consists of an axial arc in a radial magnetic field. It is conceptually identical with the cylinder discussed above. However, in the case of an arc, ion as well as electron motion must be considered. The ion Hall current and the electron Hall current will be in opposite directions. Conditions in the arc can be obtained so that the ions, which are heavier than the electrons, are only slightly affected by the magnetic field. The ion Hall current is then much less than the electron Hall current.

In an arc without a magnetic field, the electric field imposes equal and opposite forces on the electrons and ions; thus, there is no total force on the plasma. In the linear Hall accelerator, the electric field force on the electrons is opposed by the magnetic field while the ions are practically unaffected by the magnetic field. There is, thus, an unbalanced force in the direction of ion motion and the plasma is accelerated in this direction (ref. 3).

Several investigators have studied the Linear Hall Accelerator. However, their measurements have been concerned mostly with the variation of electric field with magnetic field (refs. 4, 5, 6, and 7) and the variation of force with various parameters (ref. 8). A few investigators have reported some measurements of Hall currents (refs. 5 and 9); however, there have been no systematic studies of the variation of Hall currents with the various parameters.

Since the Hall current is the basic mechanism of the linear Hall accelerator, a systematic study of the Hall current is necessary to understand the operation of the device.

In this paper, both Hall current and arc voltage measurements are presented at 15, 30, and 40 microns of mercury in argon for arc voltages from 100 to 600 volts, arc currents from 4 to 40 amperes and average magnetic field strength from 12.5 to 550 gauss. Measurements were taken of Hall current and arc voltage vs arc current for various magnetic field strengths. This data was then cross plotted to give the more meaningful variation of Hall current and arc voltage with magnetic field strength for various arc currents.

The data shows that at any axial current, the Hall current increases to a maximum and subsequently decreases as the magnetic field strength is continually increased. A theory is proposed to explain the variation of Hall current with magnetic field. This theory is based on the increase of the ion slip term which results in an increase of ion rotation and thus a decrease in Hall current with increasing magnetic field.

## DEVELOPMENT OF EQUATIONS

The relationship between current density and electric field strength is given by Ohm's law

$$\vec{j} = \sigma \vec{E}$$

In the case of a discharge in a magnetic field  $\sigma$  is a tensor quantity. In equation (1), (ref. 10) Ohm's law is written with  $\sigma$  expanded in terms of  $\sigma_0$ , the conductivity in the absence of a magnetic field, the two functions  $\omega_e \tau_e$  and  $\omega_i \tau_i$  and the magnetic flux density  $B$ . As center of mass coordinates are used,  $\vec{E}'$  must be employed where  $\vec{E}' = \vec{E} + \vec{v} \times \vec{B}$ .

$$\vec{j} = \frac{\sigma_0}{(\omega_e \tau_e)^2 + \left(1 + \left(\frac{\omega_e \tau_e}{B}\right)^2 \omega_i \tau_i\right)^2} \left\{ (1 + 2\omega_e \tau_e \omega_i \tau_i) \vec{E}' \right. \\ \left. - \frac{\omega_e \tau_e}{B} (\vec{E}' \times \vec{B}) + \left[ \left(\frac{\omega_e \tau_e}{B}\right)^2 + \frac{\omega_e \tau_e \omega_i \tau_i}{B^2} (1 + 2\omega_e \tau_e \omega_i \tau_i) \right] (\vec{E}' \cdot \vec{B}) \frac{\vec{B}}{B} \right\} \quad (1)$$

$\omega_e$  and  $\omega_i$  are the cyclotron frequencies of the electrons and ions,  $\omega_e = eB/m_e$ ,  $\omega_i = eB/m_i$ .  $\tau_e$  and  $\tau_i$  are the mean time between collision of the particles, or the reciprocals of the collision frequency. Thus  $\omega\tau$  is the ratio of the rotation frequency in the magnetic field to the collision frequency of the particle. As collisions have the effect of randomizing particle motion,  $\omega\tau$  is a measure of the effect

of the magnetic field on particle motion. For high  $\omega\tau$  the particle motion is strongly influenced by the magnetic field and for low  $\omega\tau$  the particle motion is weakly influenced by the magnetic field.

In the present case  $E_r, E_\theta, v_r, B_x,$  and  $B_\theta$  are all taken as zero. Noting that as  $\sigma_0 = \frac{n_e e^2 \tau_0}{m_e}$  and for simplicity defining a function  $W$  such that  $W = \frac{(1 + 2\omega_e \tau_0 \omega_1 \tau_1) n_e}{\omega_e \tau_0}$ . The expressions for  $j_x$  and  $j_\theta$

are then

$$j_x = n_e e \left( W \frac{E'_x}{B} + v_x \right) / (1 + W^2) \quad (2)$$

$$-j_\theta = n_e e \left( \frac{E'_x}{B} - W v_x \right) / (1 + W^2) \quad (3)$$

Minus  $j_\theta$  is used, since the axial Lorentz force is  $-j_\theta B_r$ . Three other expressions can be found for  $j_\theta$  by eliminating  $E'_x, v_x$  and  $n_e$  from the above equations.

$$-j_\theta = \frac{1}{W} (j_x - n_e e v_x) \quad (4)$$

$$-j_\theta = n_e e \frac{E'_x}{B} - W j_x \quad (5)$$

$$-j_\theta = \left( \frac{E'_x}{B} - W v_x \right) / \left( W \frac{E'_x}{B} + v_x \right) \quad (6)$$

Equation (2) can be solved for  $E'_x$  yielding

$$E'_x = \frac{1 + W^2}{W} \frac{j_x B}{n_e e} - \frac{v_x}{W} \quad (7)$$

These equations are similar to those developed in reference 6, except for the figure two in the term  $1 + 2\omega_e \tau_0 \omega_1 \tau_1$ . This is a numerical

factor which depends upon the gas being considered. In the experiment  $j_{\theta}$ ,  $j_x$ ,  $B$  and arc voltage were measured. In the interpretation of results the variation of  $j_{\theta}$  with  $B$  is explained on the basis of the variation of  $W$  with  $B$ .

## APPARATUS

A schematic of the apparatus is given in figure 1. The electrodes are 7.5 cm I.D. inserts within watercooled holders. In the present experiment, the inserts are copper at the anode and aluminum at the cathode, but these may be easily replaced by any other material. The edges of the electrodes and the glass are protected from the discharge by boron nitride insulators; these insulators leave 2.54 cm of the electrodes exposed to the discharge. The center glass is 7.3 cm I.D. The discharge length is 22.86 cm long. On either side of the discharge the electrode holders are connected to glass crosses. These crosses contain Hastings thermocouple vacuum gauges. The anode cross is connected to the gas input, and the cathode cross leads to the vacuum system. The cathode cross also contains a cantilever support for a Bakelite rod, which in turn supports an iron bar in the center of the discharge. The iron bar is centered under the solenoid and is 22.9 cm long, the bar is 3.16 cm O.D. and has a 1.27 cm hole through the center. This hole contains a teflon rod which is screwed to a boron nitride insulator at the anode end and to the Bakelite rod at the cathode end. The iron bar is covered by a 38 cm pyrex tube. This cantilever arrangement was designed so that the accelerator can be mated with any type of preionizer at the anode without changing the configuration or interfering with the flow from the preionizer. The magnet solenoid is 2.8 cm long and its center is 10.16 cm from the anode

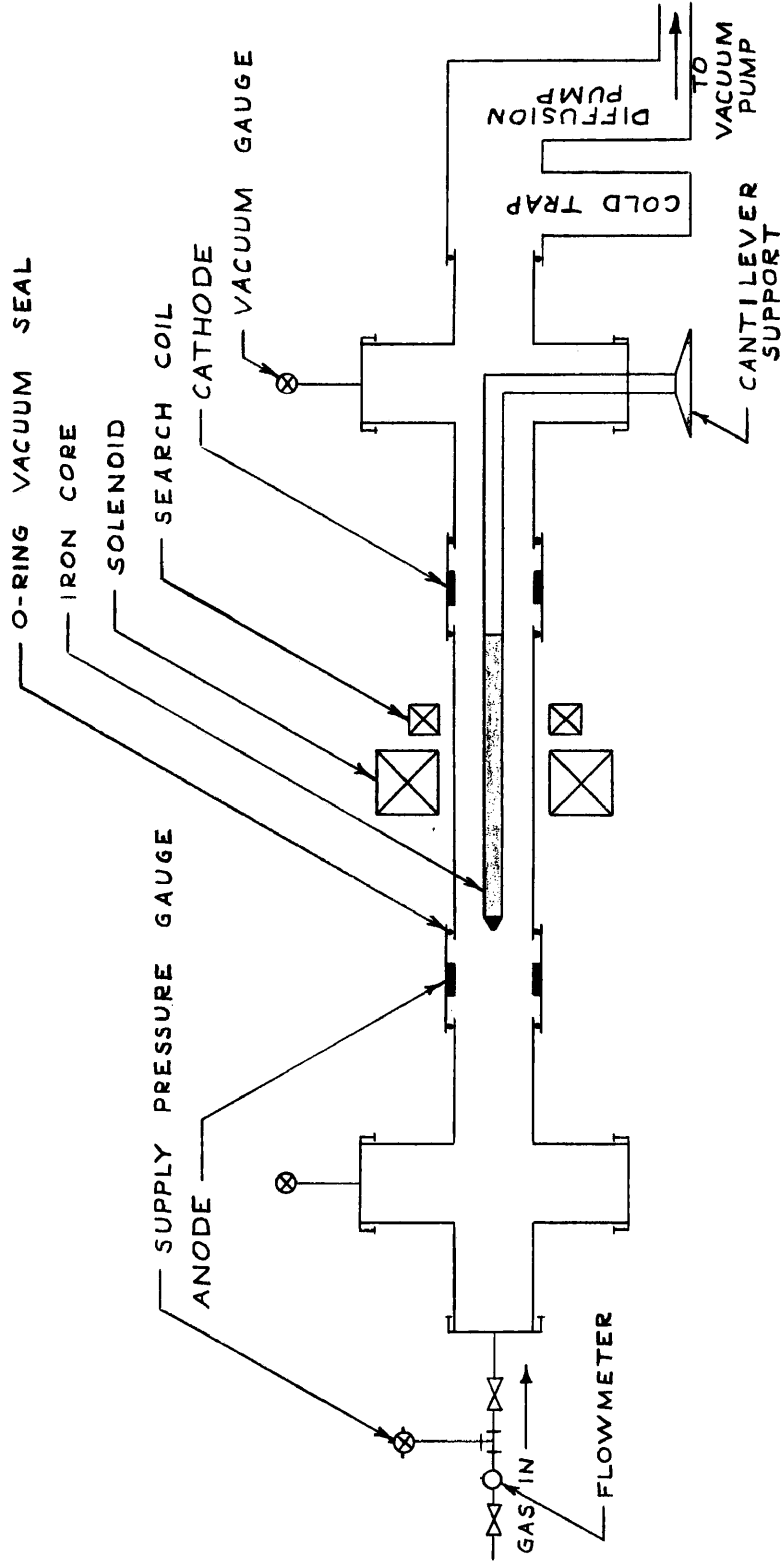


Figure 1.- Schematic of apparatus.

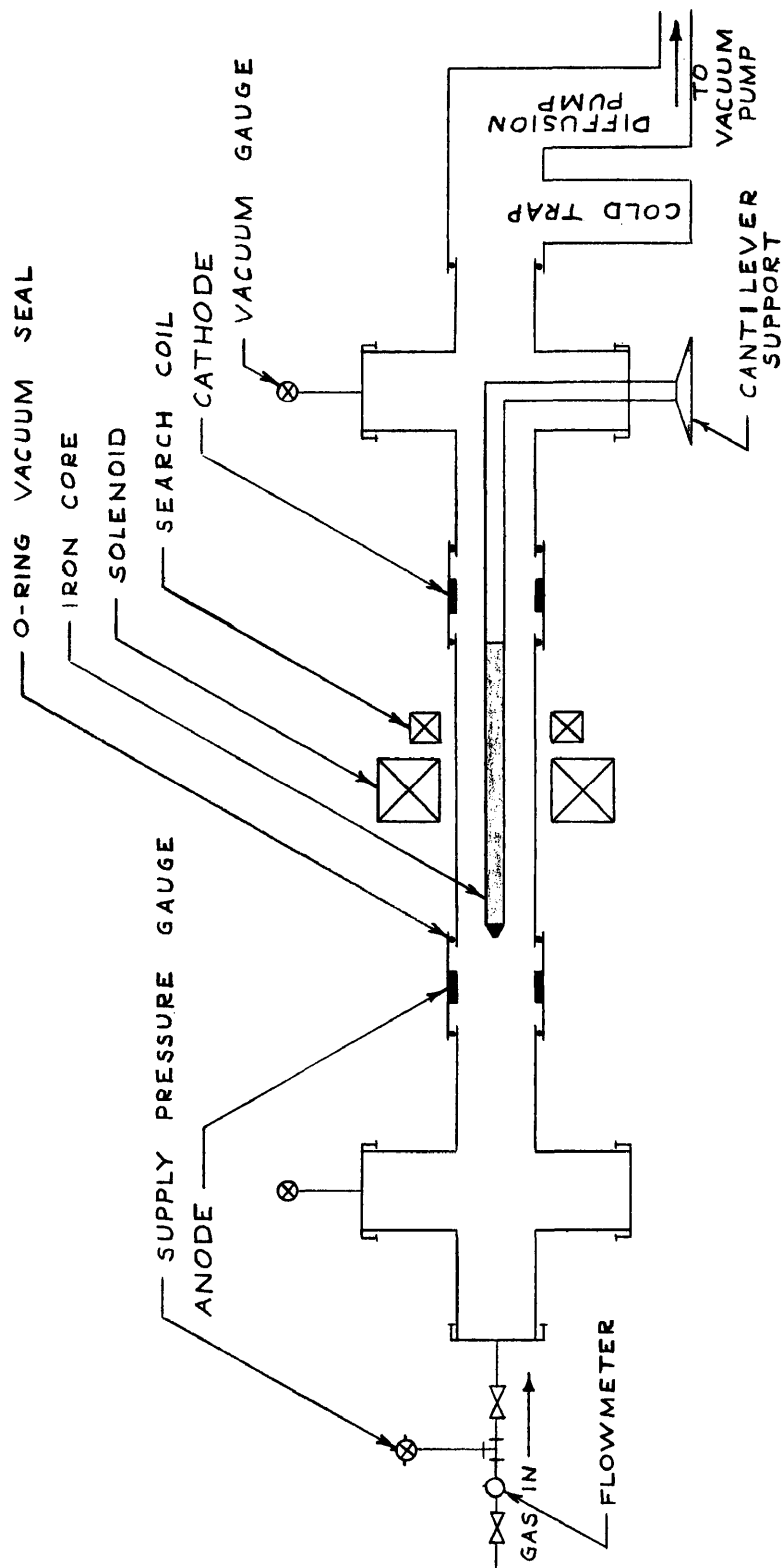


Figure 1.- Schematic of apparatus.

and 12.7 cm from the cathode. The 450 turn coil is powered by a 60-volt battery bank; the current is controlled by means of a variable resistor. A search coil is mounted 4-1/2 cm from the center of the magnet on the cathode side. This is a 100-turn coil and it is connected to a ballistic galvanometer. The arc power supply is a 700-volt 1400-ampere motor generator set and is connected to the electrodes through a 10.37 ohm ballast resistor. Figure 2 is a diagram of the magnetic field configuration for an average radial flux density of 100 gauss. A rapid increase of axial field strength occurs above 500 gauss due to saturation of the iron bar. The pumping system consists of a cold trap, a 14-inch diffusion pump and a stokes vacuum pump.

The investigations reported here are a study of the basic mechanisms of the discharge. The pumping system for the present experiments is not adequate to remove the mass flow due to high ion current. As a consequence, during operation, there is a pressure rise at the pump entrance and a pressure drop at the gas inlet. This results in a flow of neutral particles from cathode to anode. The ions are thus accelerated through the neutral gas. A new vacuum system (three 35-inch diffusion pumps) is now under construction.

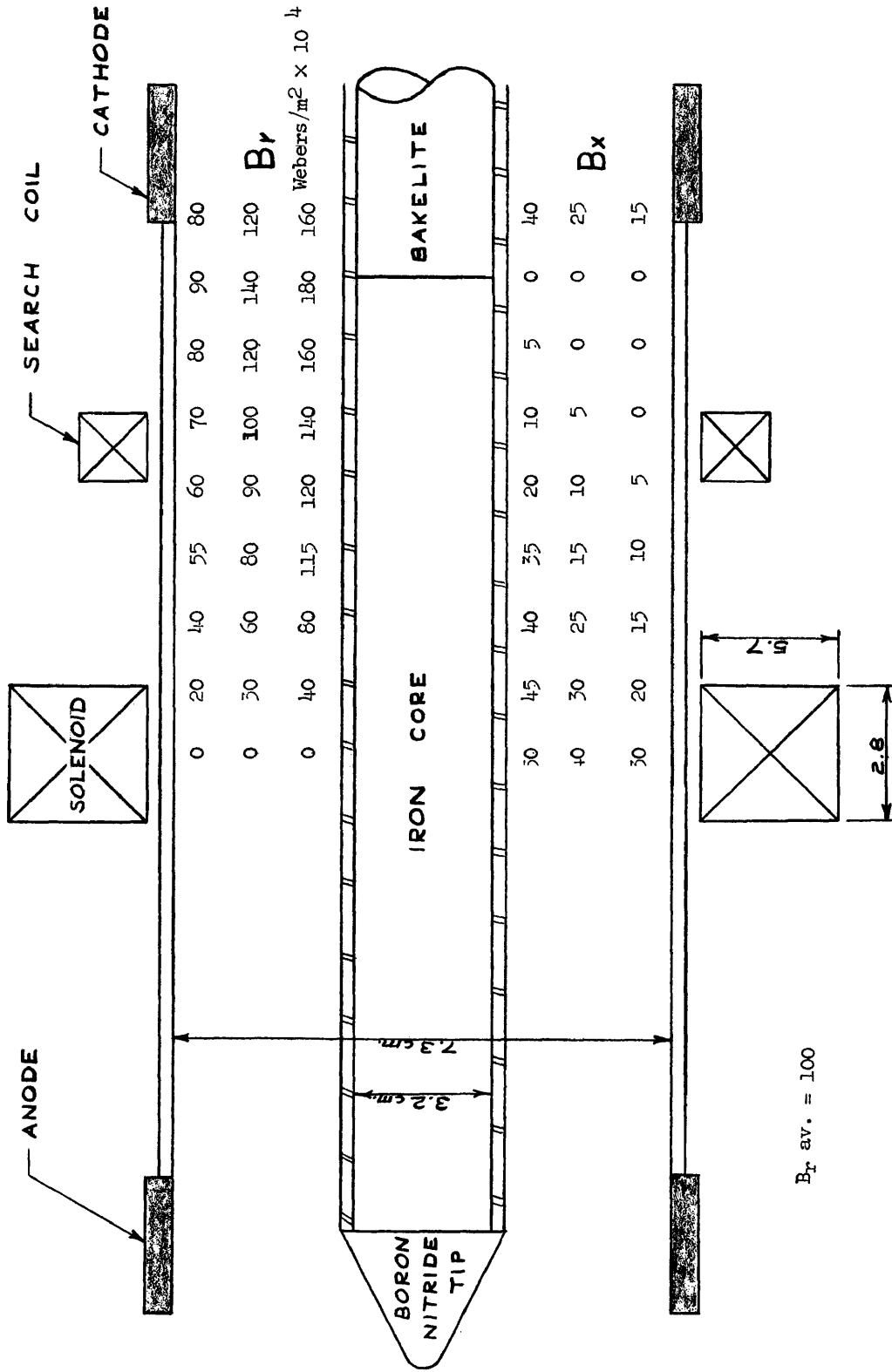


Figure 2.- Schematic of magnetic-field configuration.



## OPERATION OF DISCHARGE AND MEASUREMENTS

As the solenoid is at the center of the discharge, the radial magnetic field reverses direction from the anode to the cathode side of the discharge. This will also reverse the direction of the Hall current and of any gas rotation as these are functions of  $\vec{v} \times \vec{B}$ . However, the axial forces will remain in the same direction since these are functions of  $(\vec{v} \times \vec{B}) \times \vec{B}$ . Thus, the reversing magnetic field has the advantage of tending to destroy any gas rotation which may build up on one side of the magnet. The gas will enter the cathode side of the discharge with any rotation that has built up on the anode side, the rotating force will then be reversed and the average rotation on the cathode side should be close to zero.

The discharge for these experiments was operated with no preionizer. Thus, all ionization was supplied by the electric field. Starting ionization was supplied by a Tesla coil, but this was turned off before any measurements were taken. Voltage and current were monitored on standard meters and also recorded on a Consolidated Electric Company oscillograph. Pressure was monitored on two Hastings thermocouple gauges and also recorded on the oscillograph. Hall current was measured by means of a 100-turn search coil (ref. 3) and ballistic galvanometer. When the discharge was turned off, the collapsing magnetic field of the Hall current induced an E.M.F. in the

search coil. The total charge induced in the search coil circuit is proportional to the original current and to the ballistic galvanometer deflection. The ballistic galvanometer was calibrated by placing two 80-turn coils in place of the Hall current. These coils were 5.3 cm in diameter and 7 cm in length. The ballistic galvanometer was calibrated by using various currents in the coils. The direction of current was reversed in the two coils to represent the Hall current. When the current was turned off, the reading on the galvanometer was taken. The calibration was retaken at several magnetic field strengths in order to check if any saturation of the iron bar was affecting the readings. A slight drop in reading noted at 550 gauss was within reading error. However, this drop and the increased axial field at 550 gauss may explain the sharp dropoff of Hall current noted at 550 gauss in the data. The ballistic galvanometer was calibrated in amperes.

The radial length between the iron core and the outer glass was 1.75 cm. The length of the Hall current region was estimated as 10.16 cm. Thus the Hall current cross sectional area was 17.78 square cm. The axial current cross sectional area was 30.59 square cm. The Hall current was consequently multiplied by  $10^4/17.78$  to give amperes per square meter, the corresponding multiplier for the axial current was  $10^4/30.59$ . The arc voltage was multiplied by 4.37 to give volts per meter. Magnetic field was calibrated vs magnet current by a gauss meter. Magnet current was set with a standard ammeter.

In operating the discharge, pressure was set using a variable leak; the voltage across the electrodes and the magnetic field were

preset. The discharge was started with the Tesla coil and when voltage and current oscillations (as observed on the meters) had damped out, the oscillograph was started and the switch controlling the ballistic galvanometer was depressed. The discharge was then turned off and the reading on the ballistic galvanometer was taken. Ideally, it would be desirable to operate the discharge at constant current for various magnetic field strengths. However, as the power supply was not current controlled, it was difficult and time consuming to adjust the current during each run. At each magnetic field strength the discharge was started at a series of voltages so that a series of currents could be obtained. After preliminary data reduction, more data were taken in regions of interest. In order to extend the range of currents at high magnetic field strengths, it was sometimes necessary to start the discharge and then adjust the voltage downward. Data were taken at 15, 30, and 40 microns and those data are presented in the form of arc voltage in volts per meter and Hall current in amperes per square meter plotted vs arc current in amperes per square meter for various magnetic field strengths.

The data was then cross plotted to give arc voltage and Hall current vs magnetic field strength for various arc currents. These curves are presented in figures 3 through 6.

Several measurements which are desirable for a more complete analysis are now being undertaken. A program has been started to measure local voltage drop with floating probes and to make some measurements of ion density and electron temperature with Langmuir and

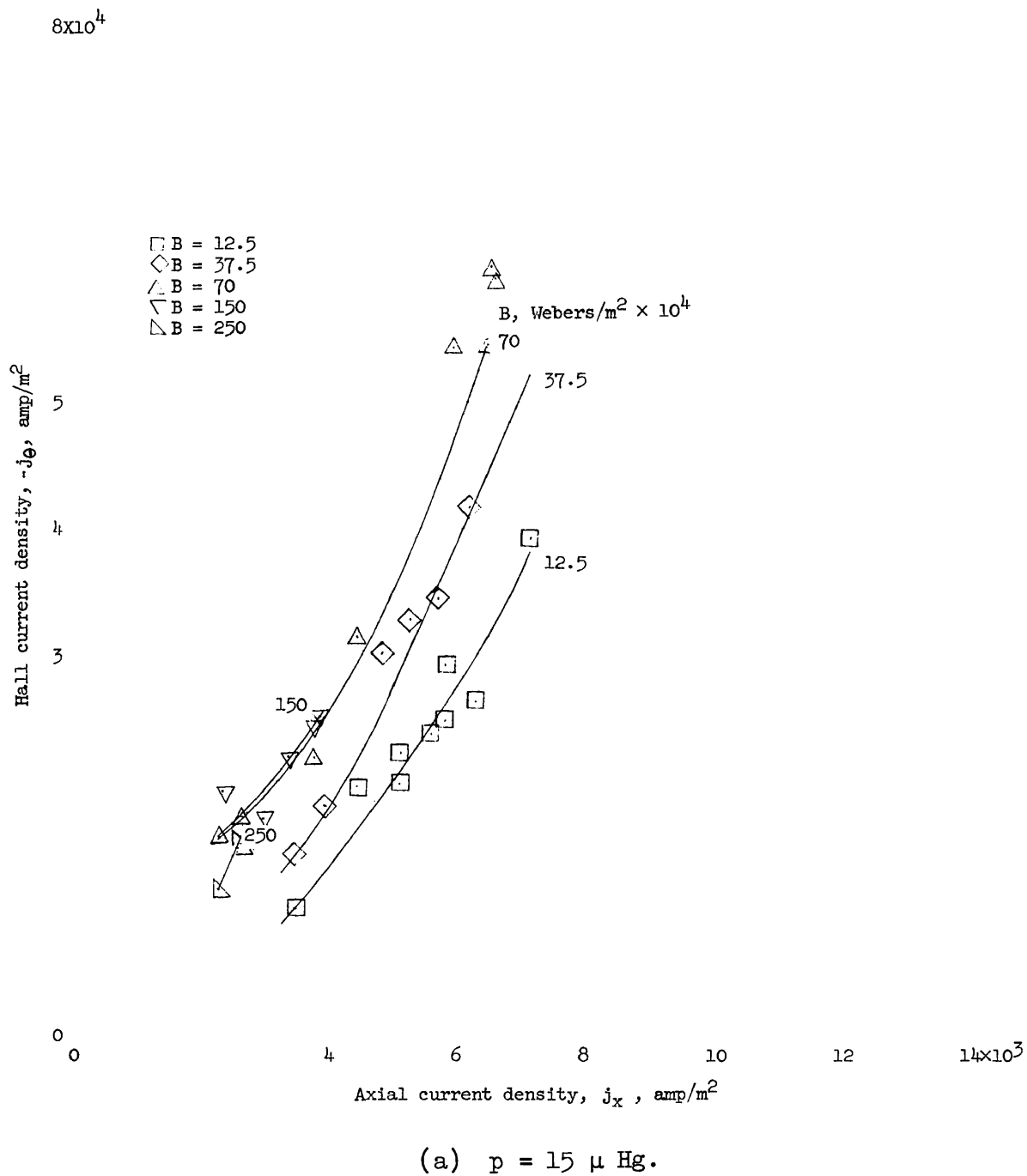
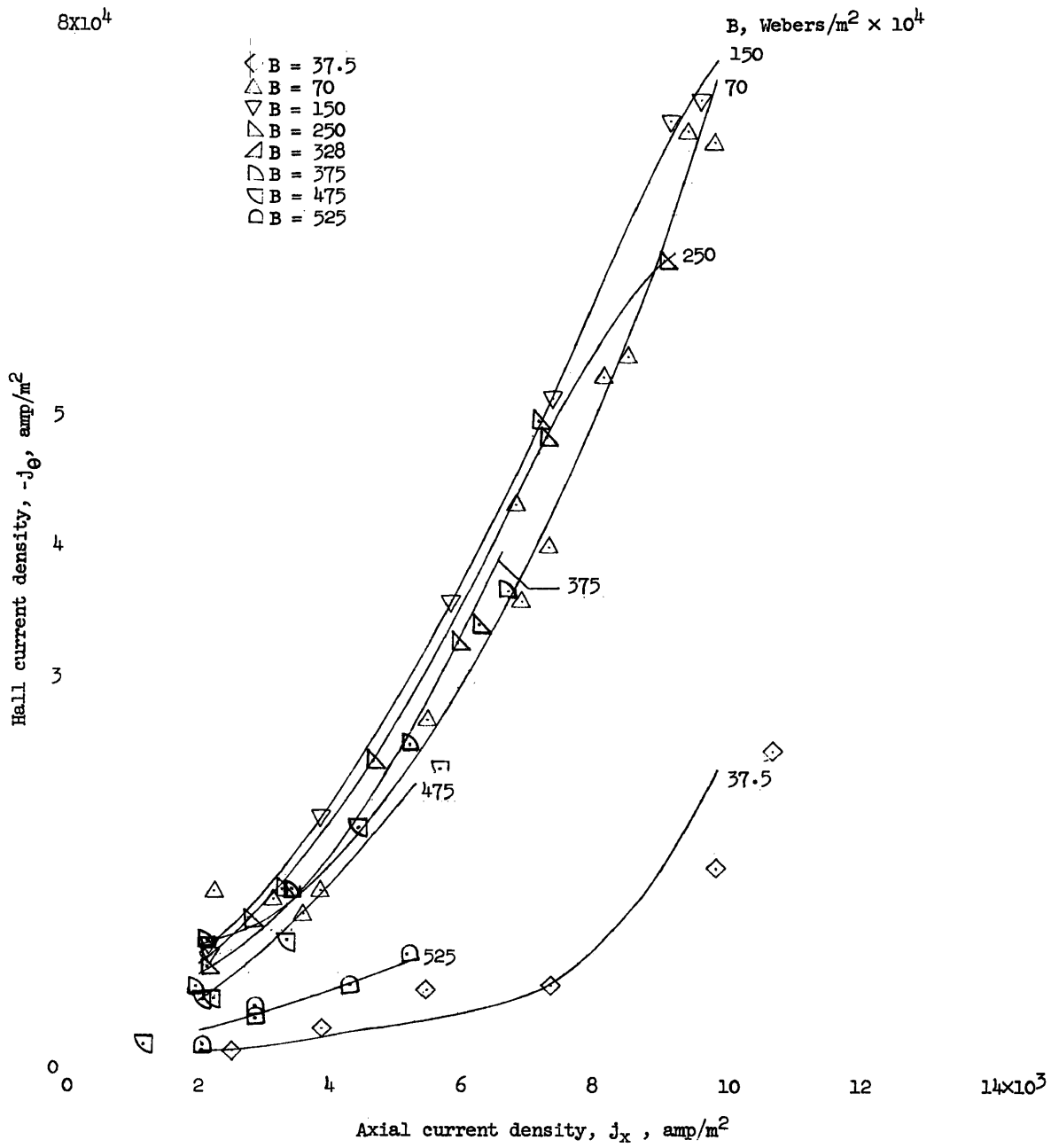
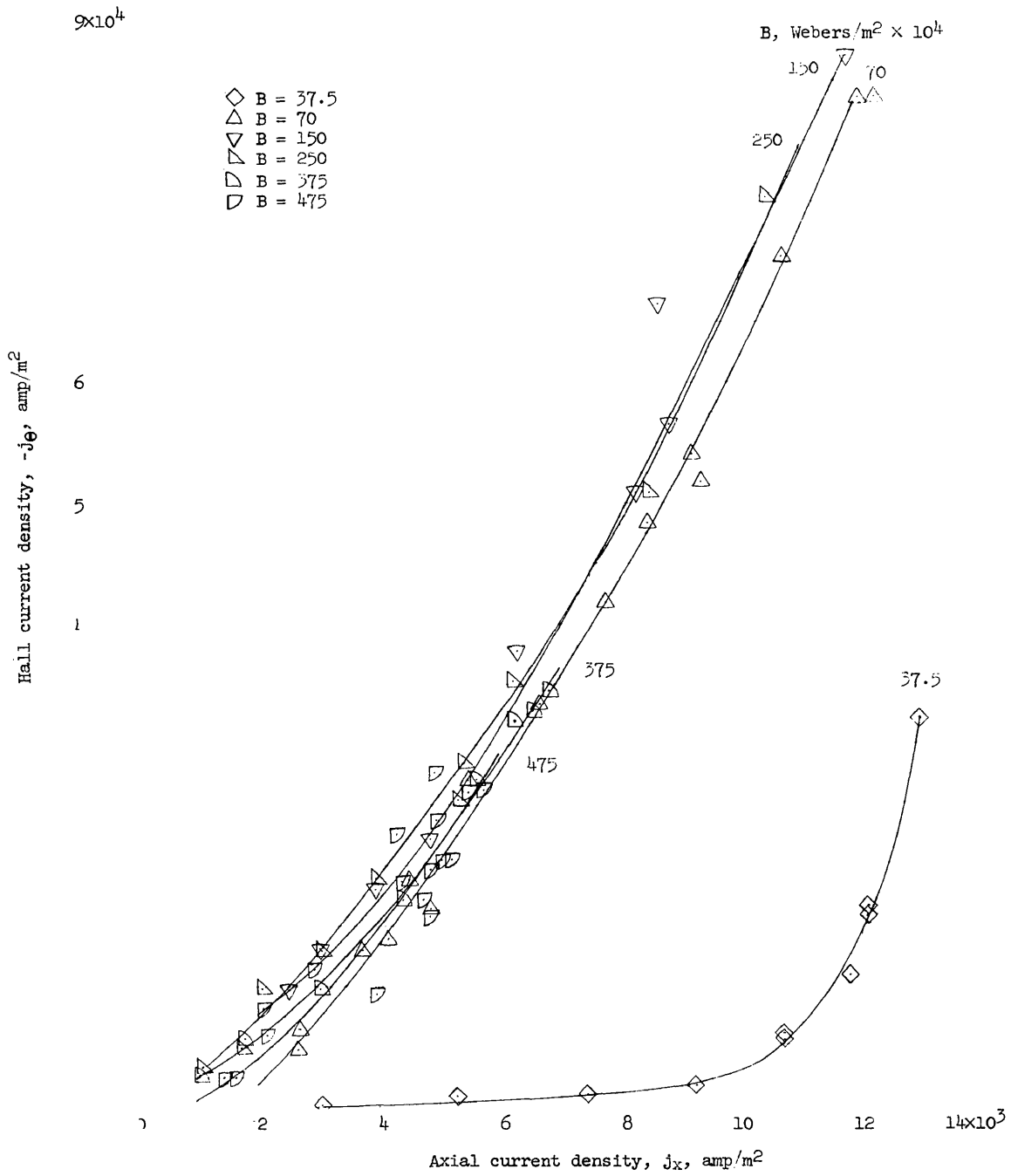


Figure 3.- Hall current density versus axial current density for various magnetic flux densities.



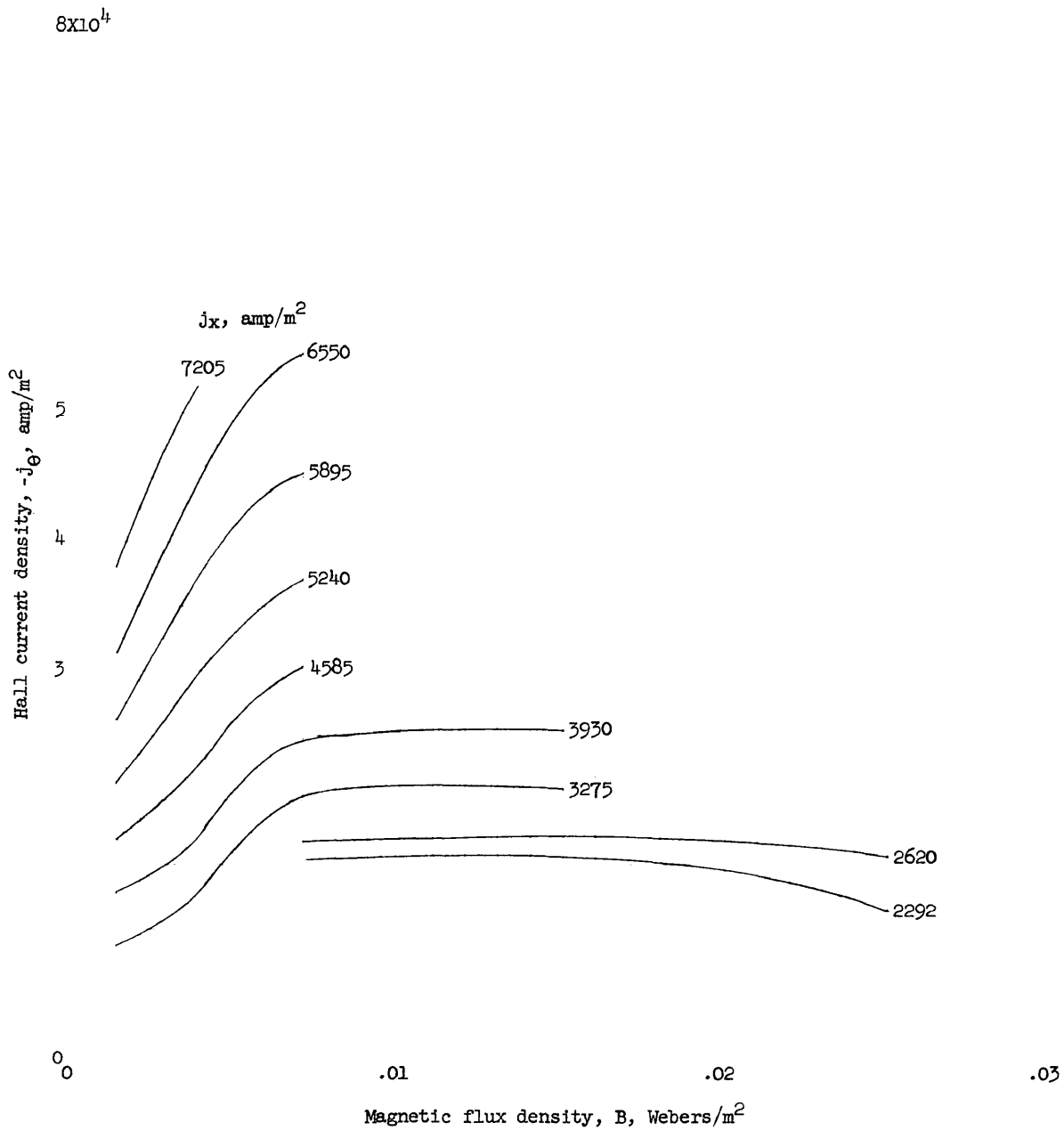
(b)  $p = 30 \mu \text{ Hg}$ .

Figure 3.- Continued.



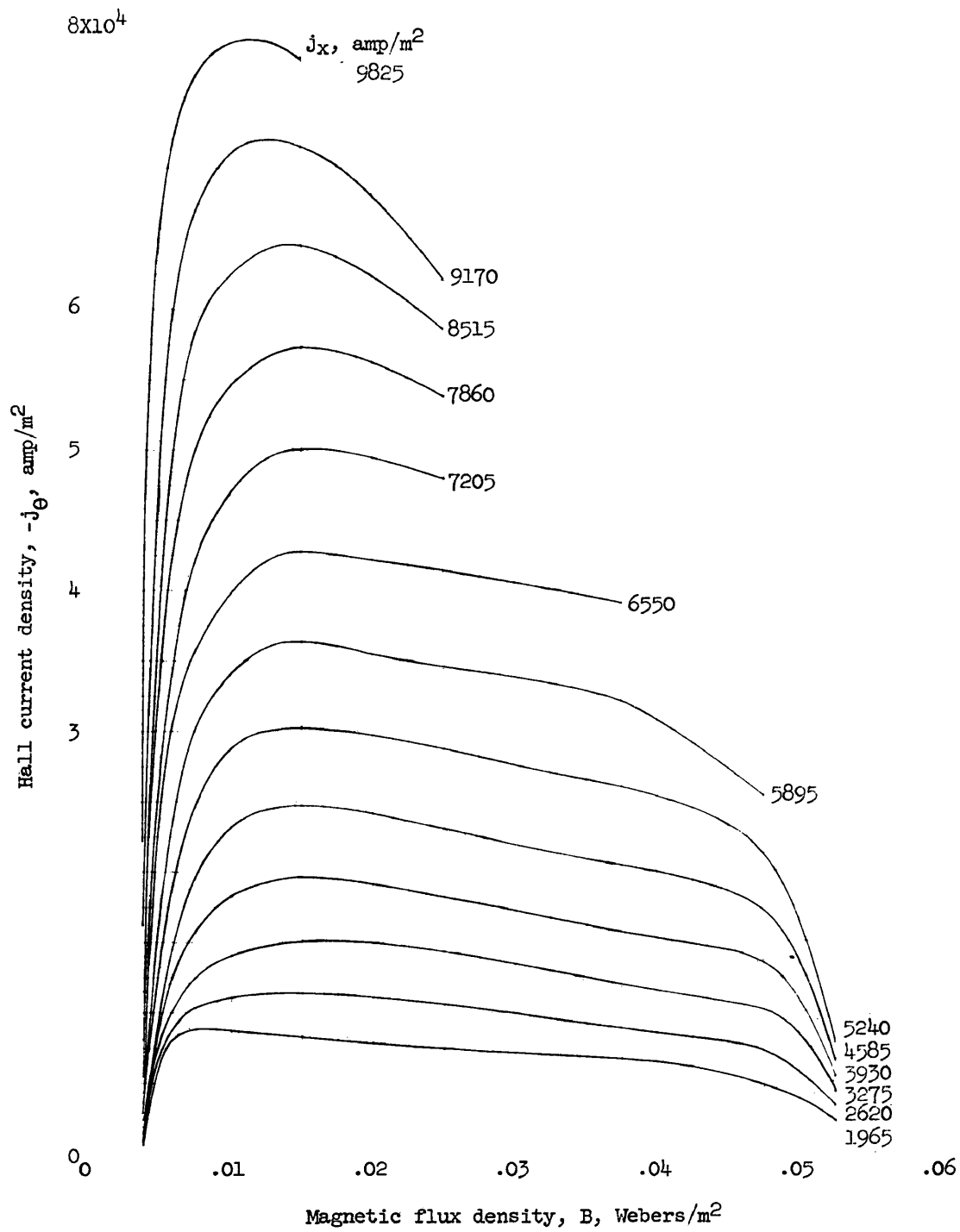
(c)  $p = 40 \mu \text{ Hg}$ .

Figure 3.- Concluded.



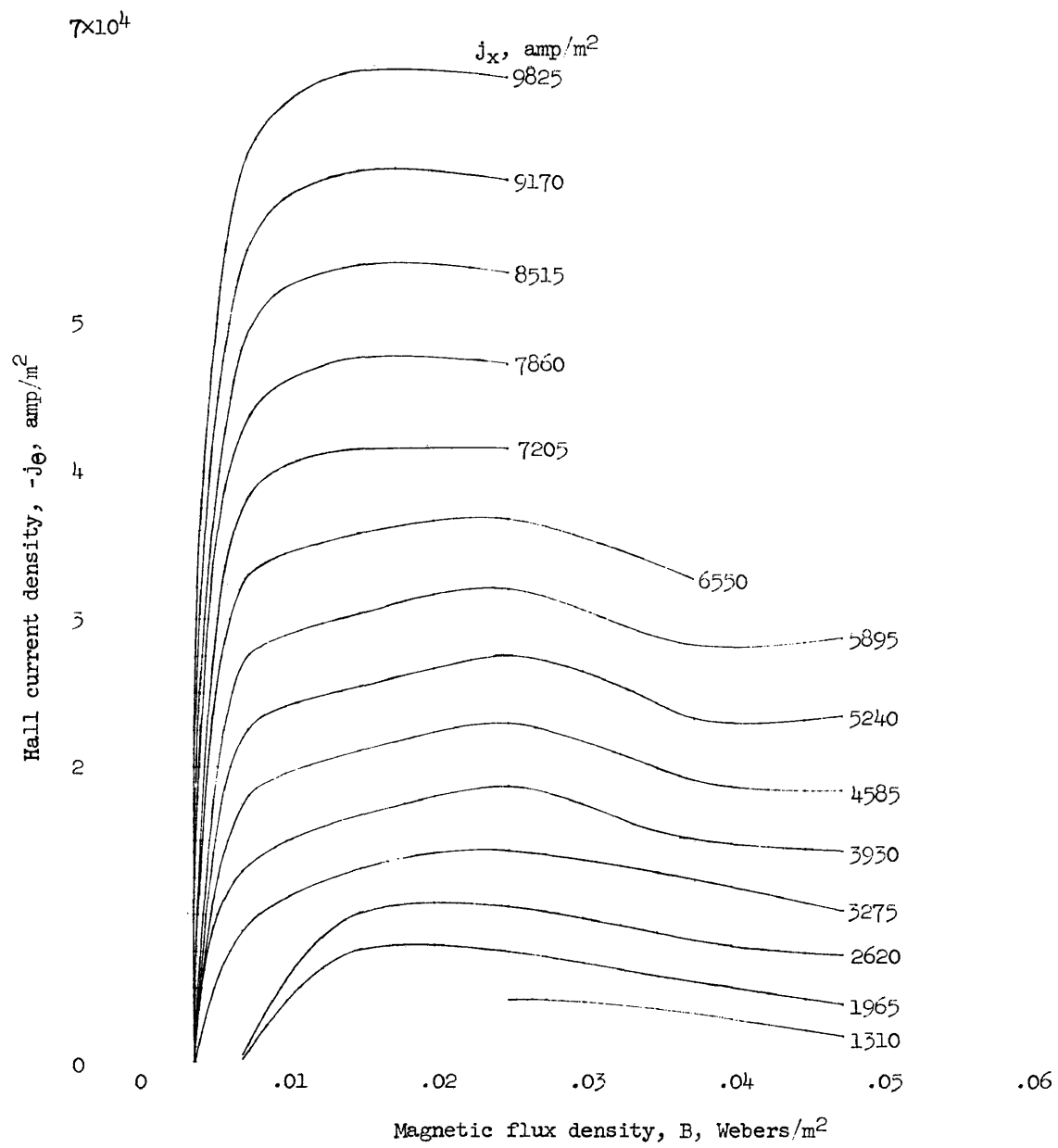
(a)  $p = 15 \mu \text{ Hg}$ .

Figure 4.- Hall current density versus magnetic flux densities for various axial current densities.



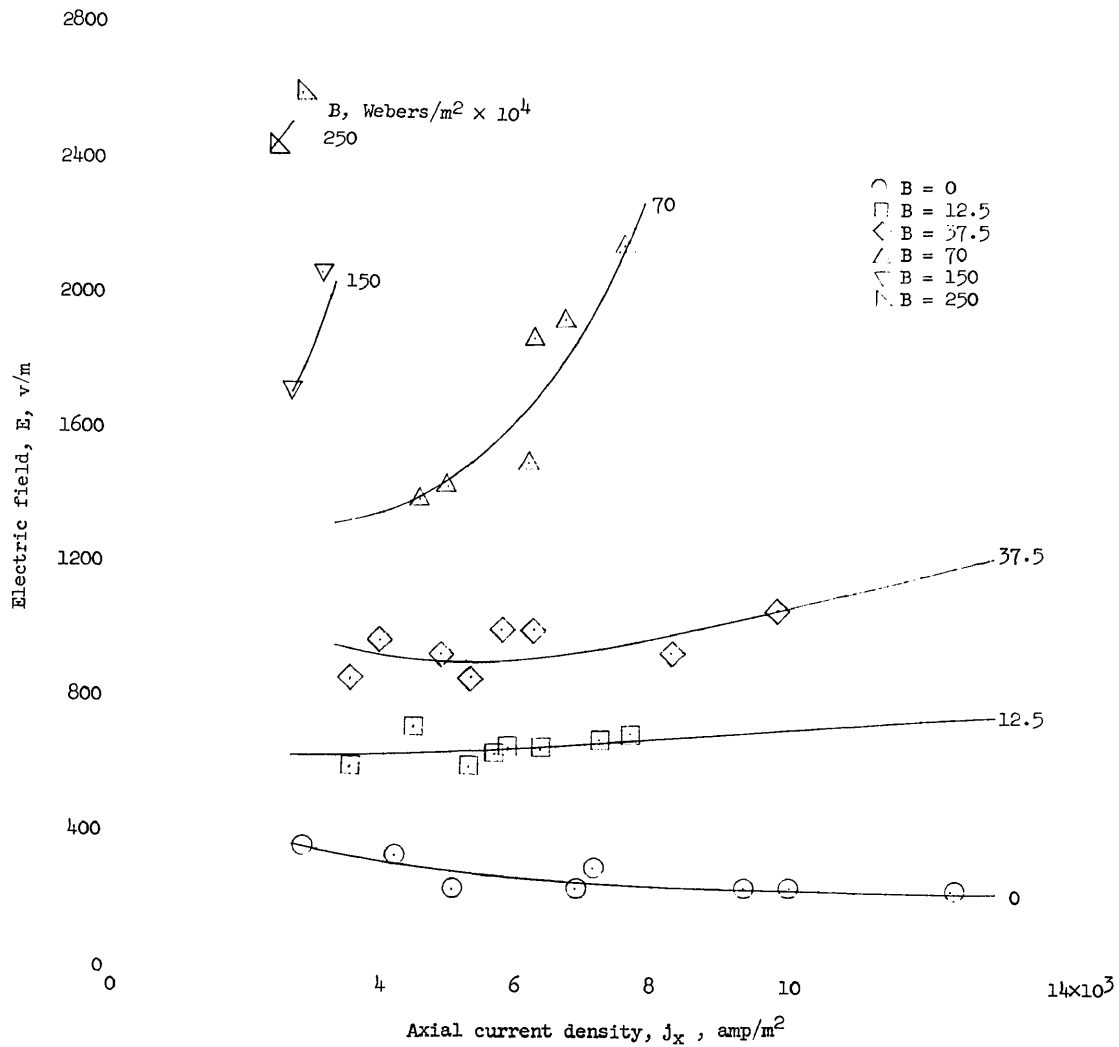
(b)  $p = 30 \mu \text{ Hg}$ .

Figure 4.- Continued.



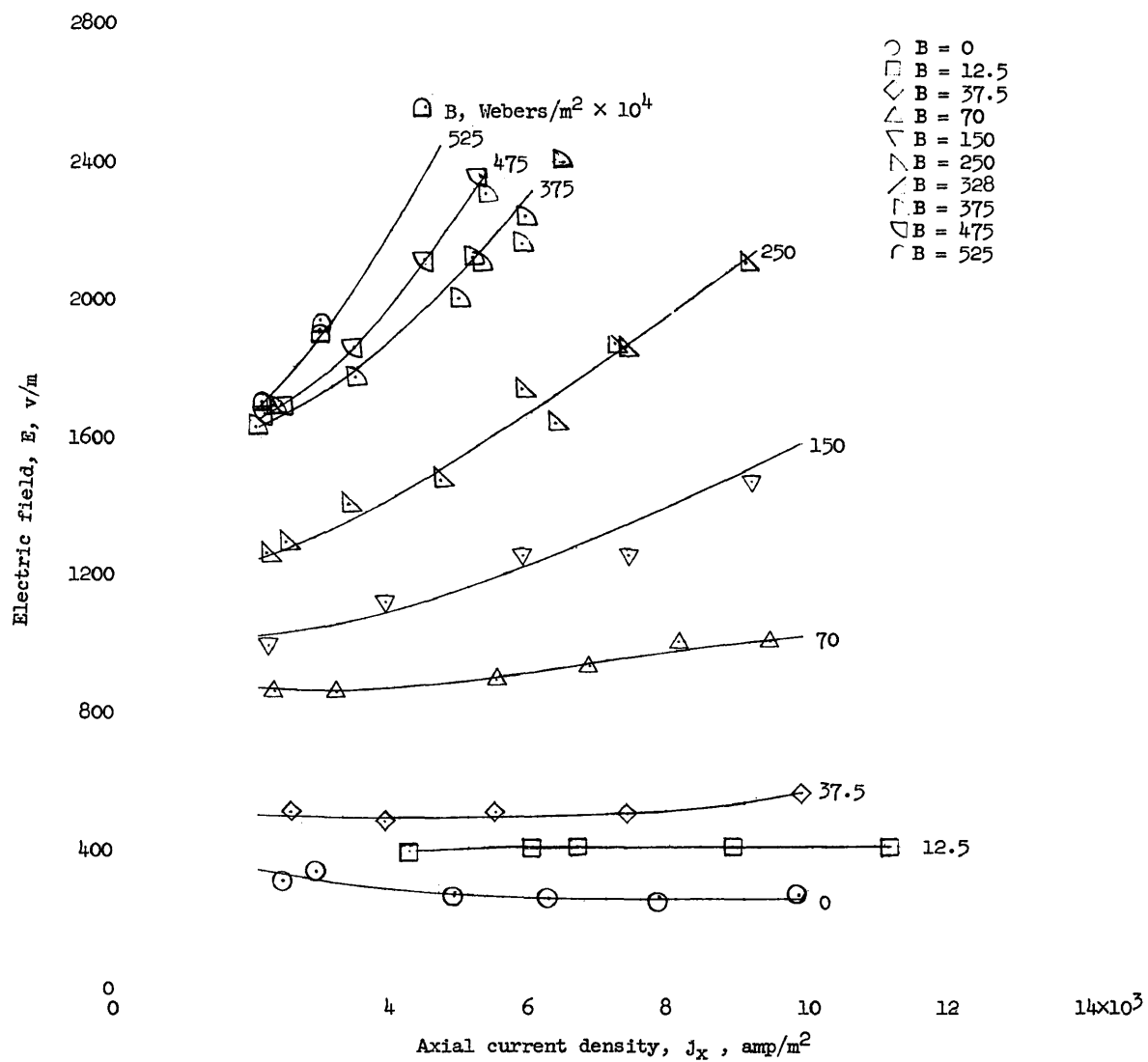
(c)  $p = 40 \mu \text{ Hg}$ .

Figure 4.- Concluded.



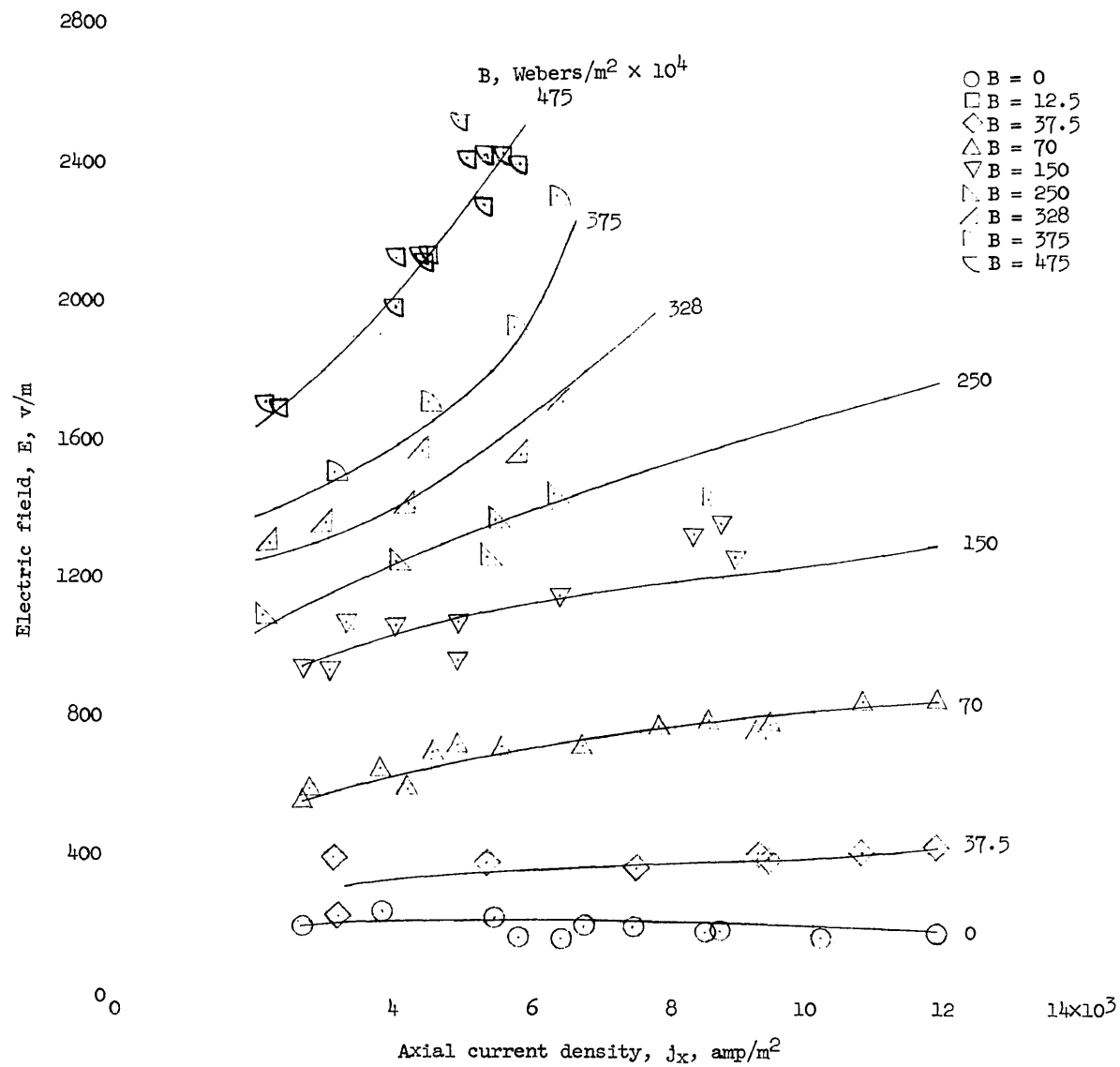
(a)  $p = 15 \mu \text{ Hg}$ .

Figure 5.- Electric field versus axial current density for various magnetic flux densities.



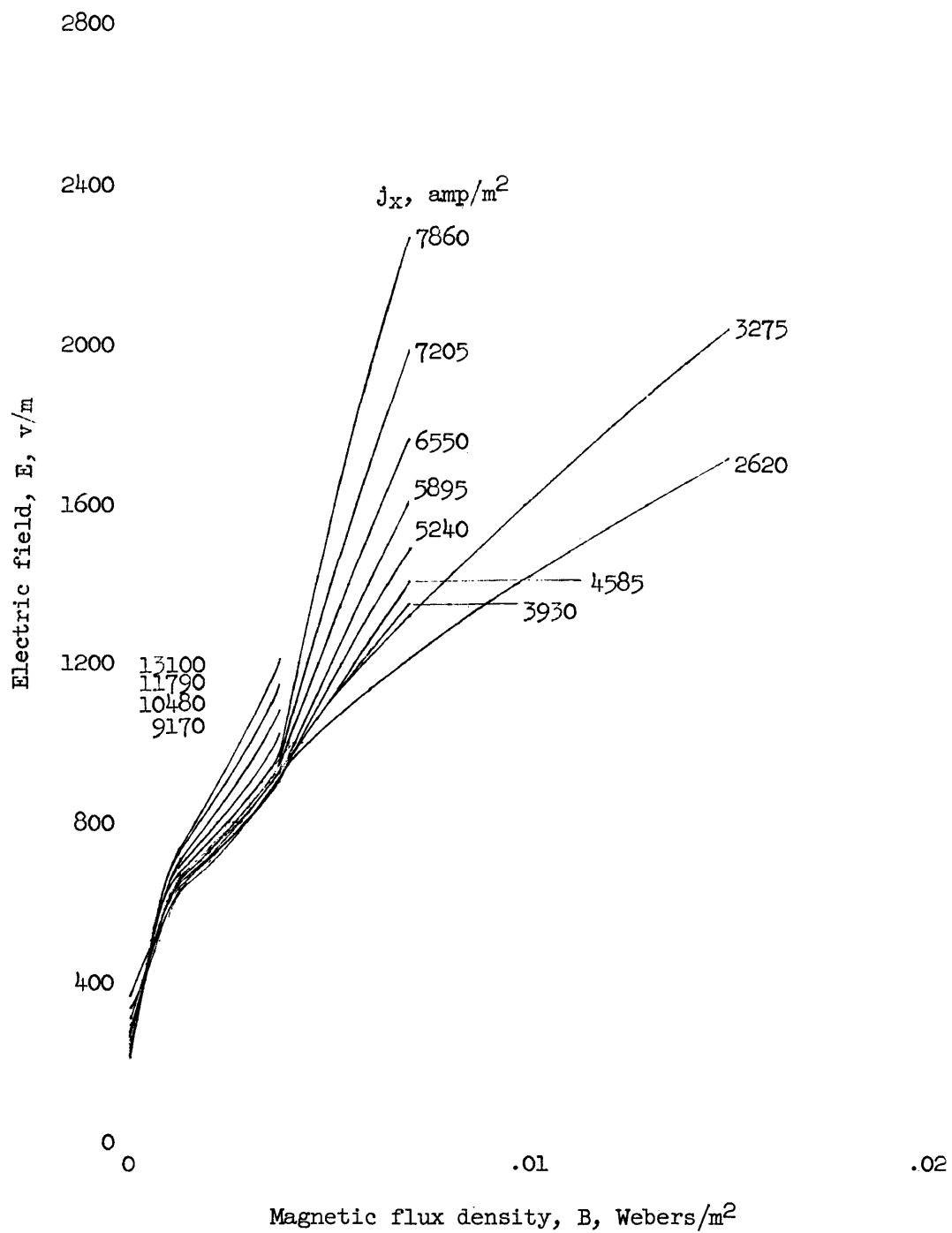
(b)  $p = 30 \mu \text{ Hg}$ .

Figure 5.- Continued.



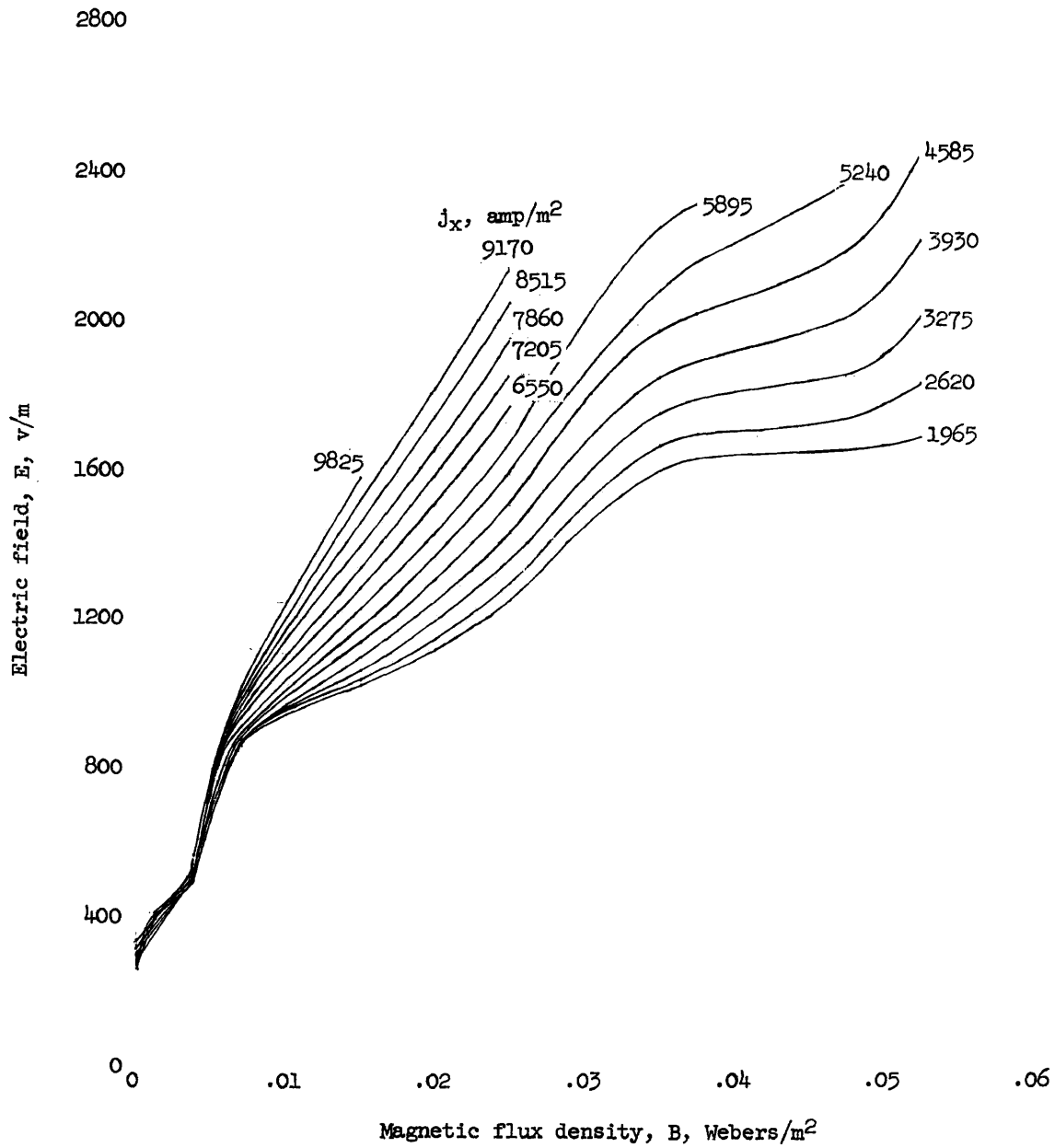
(c)  $p = 40 \mu \text{ Hg}$ .

Figure 5.- Concluded.



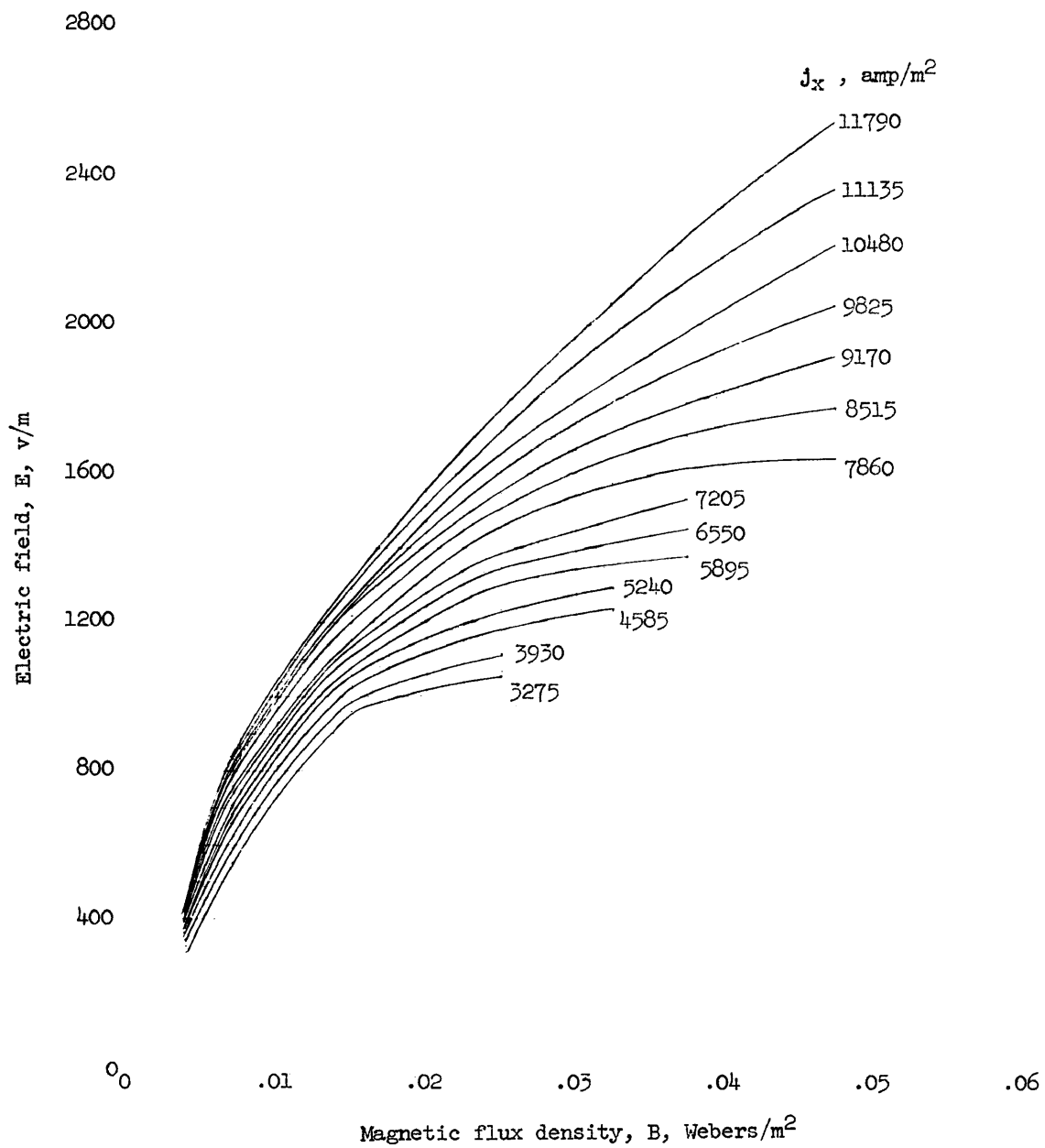
(a)  $p = 15 \mu Hg$ .

Figure 6.- Electric field versus magnetic field strength for various axial current densities.



(b)  $p = 30 \mu \text{ Hg}$ .

Figure 6.- Continued.



(c)  $p = 40 \mu \text{Hg}$ .

Figure 6.- Concluded.

double probes. The floating probe errors should cancel if the probes are sufficiently close together so that the plasma conditions are the same at both locations. However, the magnetic field will influence the electron temperature and ion density measurements to some extent (ref. 11). The sense of variation of these parameters should be measurable at any constant magnetic field strength, but there is some question in comparing measurements taken at different magnetic field strengths. Attempts will also be made in the future to measure velocities and forces in the accelerator.

A few crude measurements of oscillations in the discharge have been made with a simple metal plate capacitively coupled to the discharge through the glass. However, no survey of this parameter has been taken as yet.

### INTERPRETATION OF RESULTS

The most striking result found is the increase to a maximum and subsequent decrease of Hall current with increase of magnetic field at constant axial current. The increase of the Hall current with increasing axial current at constant magnetic field is expected and the form of the arc voltage versus axial current curves at constant magnetic field has been previously reported (ref. 3). The shape of the curves of arc voltage versus magnetic field strength observed here are different from those normally reported (refs. 4, 5, 6, 7), but this may be due to the inherent errors in measuring total arc voltage rather than local electric field, or it may be due to our particular operating conditions.

The complete equation for  $j_\theta$  (eq. (4)) including the motion of ions and neutral particles but excluding any turbulent effects is:

$$-j_\theta = \frac{1}{W} (j_x - n_e e v_x)$$

The inclusion of  $2n_e v_e \omega_i \tau_i$  in the term

$$W = \frac{1 + 2n_e v_e \omega_i \tau_i}{\omega_e \tau_e}$$

gives the influence of ion slip. The ion slip term will increase  $W$  and therefore, decrease  $j_\theta$  at constant  $j_x$ . Repeating equation (7)

for  $E'_x$

$$E'_x = \frac{1 + W^2}{W} \frac{j_x B}{n_e e} - \frac{v_x B}{W}$$

The effect of ion slip on  $E'_x$  is seen to be more complicated.

Considering the term

$$\frac{1+W^2}{W} = \frac{1}{W} + W = \frac{\omega_e \tau_e}{1 + 2n_e \tau_e \omega_1 \tau_1} + \frac{1 + 2n_e \tau_e \omega_1 \tau_1}{\omega_e \tau_e} \quad (8)$$

for  $W \ll 1$ , an increase in  $\omega_1 \tau_1$  will decrease  $E'_x$  (through increase in ion current) while for  $W \gg 1$  an increase in  $\omega_1 \tau_1$  will increase  $E'_x$ . For constant  $j_x$  the increase then subsequent decrease of  $-j_y$  is due either to variations of  $W$ ,  $v_x$ , or  $n_e$  with  $B$ . At the particular operating conditions considered here,  $n_e e$  is probably small and  $v_x$  the center of mass velocity is, as pointed out in the apparatus section, limited by the pumping system. It seems for the present case, that the effect of  $n_e e v_x$  can be neglected.

A simple explanation of the variation of Hall current with magnetic field at constant  $j_x$  can be based on the variation of  $W$  with magnetic field. The following assumptions were made, firstly, that  $n_e e v_x$  was negligible compared to  $j_x$  and secondly, that  $\tau_e$  and  $\tau_1$  were constant for  $j_x$  constant. This second assumption is based on the condition that  $\tau_e$  and  $\tau_1$  are not explicit functions of  $E'_x$  or  $B$ . The calculated values of  $\frac{\omega_e \tau_e}{B}$  and  $\frac{\omega_1 \tau_1}{B}$  in the literature usually depend on equality of electron and ion temperatures (ref. 8). Our low pressure operation does not justify this assumption.

If, for  $j_x$  constant,  $\tau_e$  and  $\tau_1$  are also constant  $W$  will be a function of  $B$  only as seen in the following equation:

$$W = \frac{1}{\frac{e}{m_e} \tau_e B} + 2 \frac{e}{m_1} \tau_1 B \quad (9)$$

Thus

$$\frac{dW}{dB} = -\frac{1}{\frac{e}{m_e} \tau_e B^2} + \frac{2e}{m_1} \tau_1 \quad (10)$$

and

$$\frac{d^2W}{dB^2} = \frac{2}{\frac{e}{m_e} \tau_e B^3} \quad (11)$$

Hence  $W$  will have a minimum value at

$$\frac{2e}{m_e} \tau_e B \frac{e}{m_1} \tau_1 B = 1 \text{ or, } 2\omega_e \tau_e \omega_1 \tau_1 = 1 \quad (12)$$

At this minimum value

$$W_{\min} = \frac{2}{\omega_e \tau_e} \quad (13)$$

and

$$\left[ 2\omega_1 \tau_1 = \frac{1}{\omega_e \tau_e} \right] W = W_{\min} \quad (14)$$

In order to generate some theoretical curves for  $j_\theta$  versus  $B$  equation (4) is rewritten in the form

$$W = \frac{j_x}{-j_\theta} \quad (15)$$

For a particular experimental curve a calculation was made of the minimum value of  $W$ , i.e.,  $W_{\min} = \frac{j_x}{-j_{\theta \max}}$ . The values of  $\omega_e \tau_e$  and  $\omega_1 \tau_1$  were then calculated for this case using equations (13) and (14).

These values were then divided by the magnetic field strength at the maximum  $j_{\theta}$  point. The resultant values of  $\frac{\omega_e \tau_e}{B}$  and  $\frac{\omega_1 \tau_1}{B}$  were used with equation (10) to calculate  $W$  as a function of  $B$ . Typical plots of  $1/W$  and  $(1 + W^2)/W$  versus  $B$  are given in figure 7. Equation (7) was used to calculate values of  $n_e e E'_x$  versus  $B$ . The sheath voltage was assumed to be equal to the experimental voltage at  $B = 0$  and it was also assumed that  $n_e$  was constant for constant  $j_x$ . A value of  $n_e$  was chosen so that the highest point of the experimental and theoretical  $E'_x$  versus  $B$  curves would match and the assumed sheath voltage was added to the theoretical curves so that the bottom points would also match. Thus, only the shape of these curves can be compared. The method of calculating the  $W_{min}$ , of course, forces the experimental and theoretical Hall current curves to match at  $-j_{\theta}$  max. In figure 8, experimental and theoretical curves of  $j_{\theta}$  versus  $B$  are compared for  $j_x = 3930, 5240,$  and  $9170$  amperes per square meter; at  $j_x = 3930$  amperes per square meter,  $W_{min} = 0.2, B = 0.015$  weber per square meter,  $\omega_e \tau_e / B = 668, \omega_1 \tau_1 / B = 3.32$ ; at  $j_x = 5240, W_{min} = 0.1158, B = 0.015,$   $\omega_e \tau_e / B = 772, \omega_1 \tau_1 / B = 2.9$ ; at  $j_x = 9170, W_{min} = 0.1274, B = 0.125,$   $\omega_e \tau_e / B = 1256, \omega_1 \tau_1 / B = 2.55$ . In figure 9 the theoretical and experimental curves of  $E'_x$  versus  $B$  are compared for  $j_x = 5240$  at 30 microns mercury 247 volts per meter have been added to the theoretical curves to represent sheath voltage, and for proper curve matching  $n_e$  was adjusted to be  $2.67 \times 10^{18}$  particles per meter<sup>3</sup>. This corresponds to a reasonable percent ionization. The Hall current curves match quite well and seem off by only a slight rotation. This may be due to the error involved in neglecting  $n_e e v_x$  when calculating  $W_{min}$ . The  $E'_x$  curve

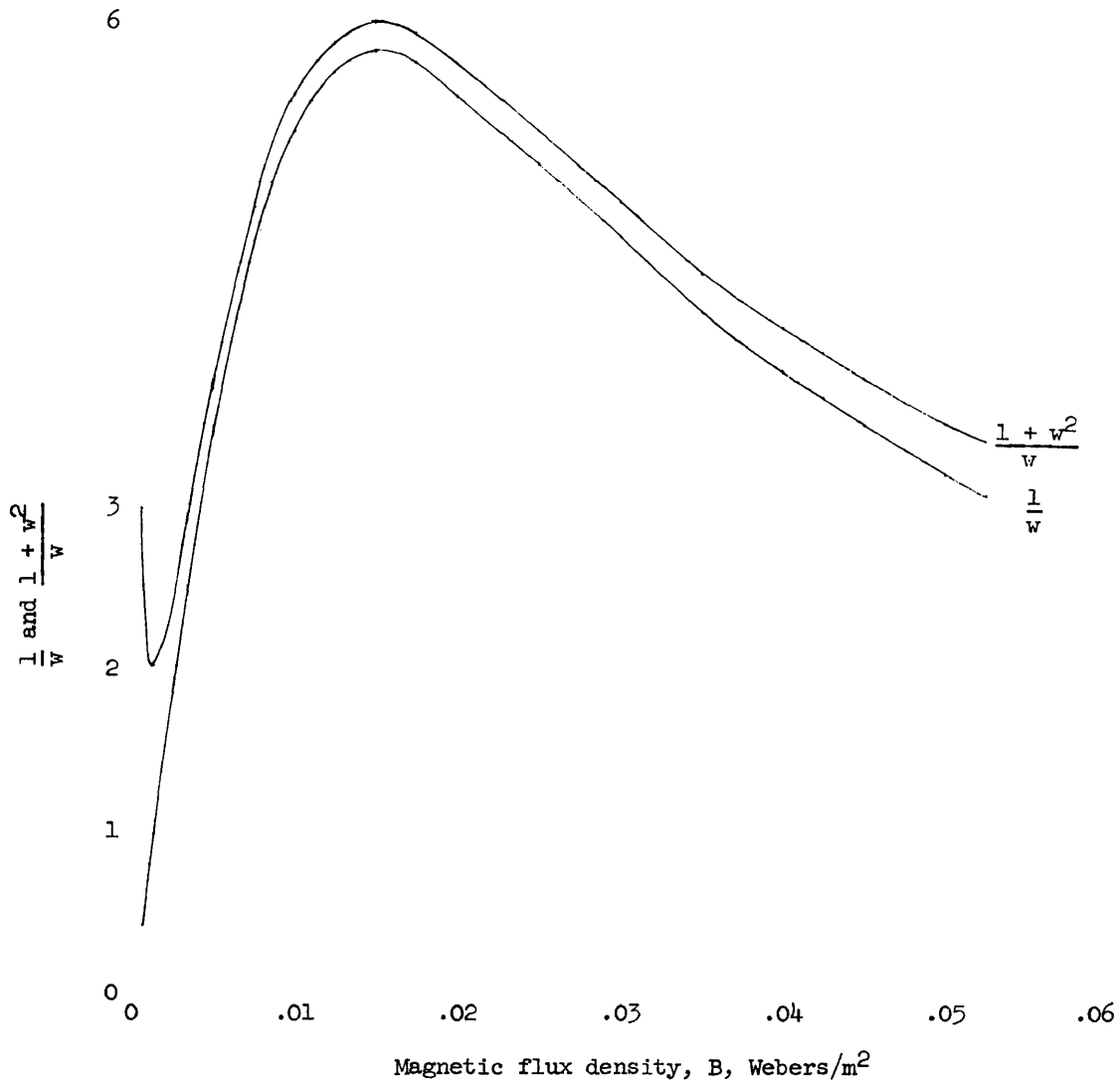


Figure 7.- Variation of  $\frac{1}{w}$  and  $\frac{1+w^2}{w}$  with magnetic flux density.  
( $p = 30 \mu \text{ Hg.}$ )

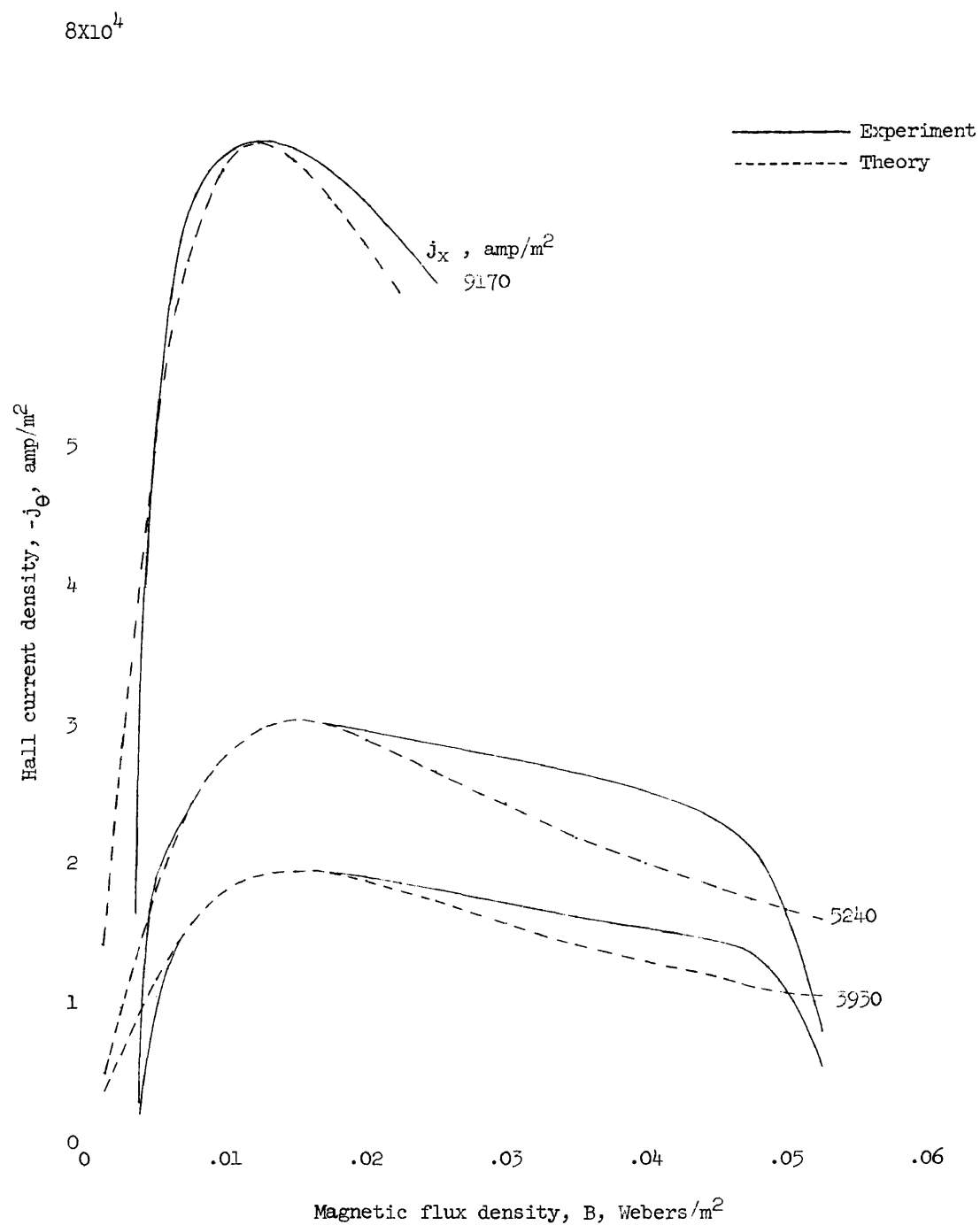


Figure 8.- Comparison of theory and experiment (Hall current density versus magnetic flux density).  $p = 30 \mu \text{ Hg}$ .

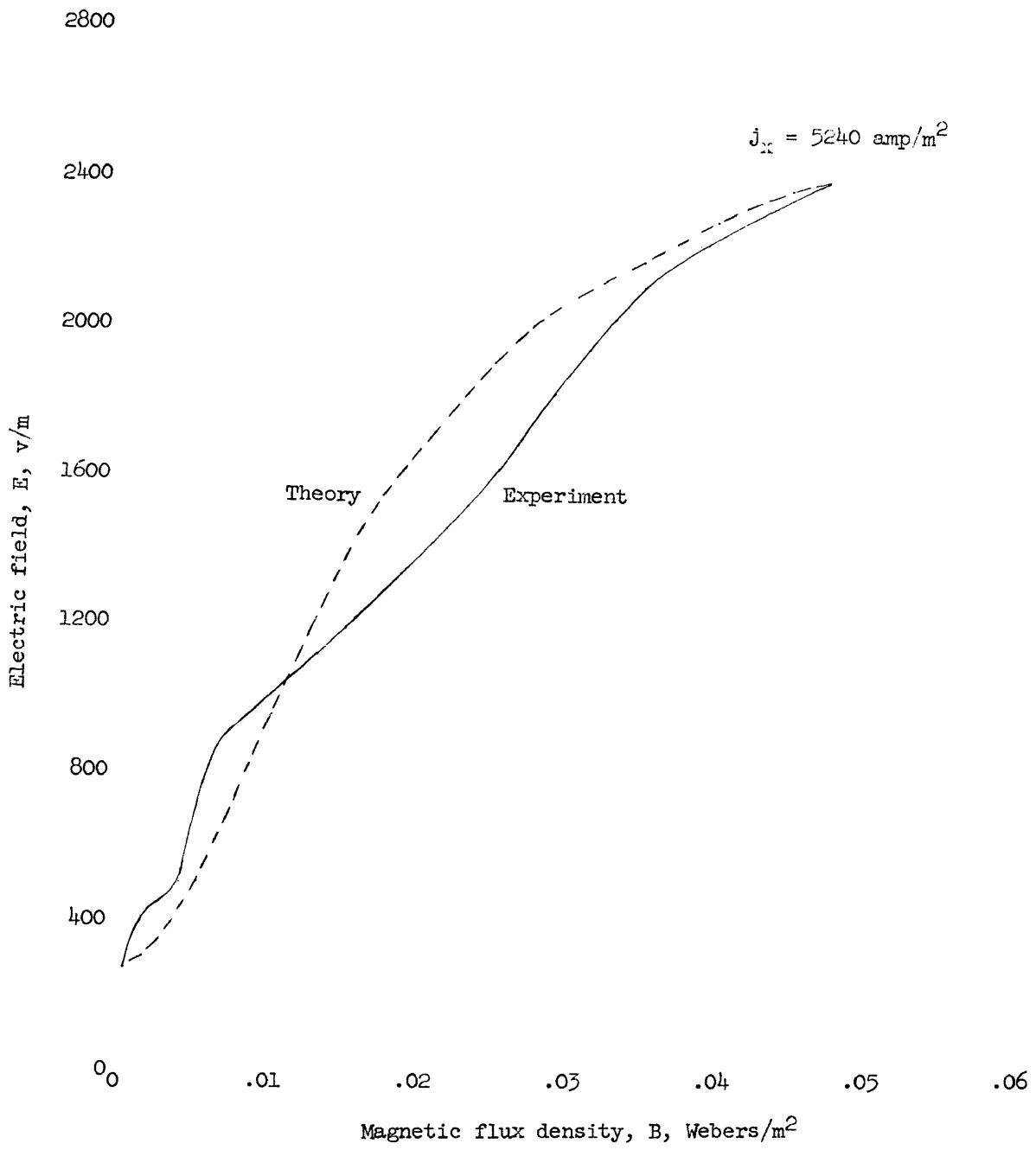


Figure 9.- Comparison of theory and experiment (electric field versus magnetic flux density).

does not match as well except at the high magnetic field strengths where the general curvature is the same.

In matching theory with experiments, it should be noted that the values for  $E'_x$  in figures 5 and 6 are based on averaging the voltage drop over the length of the apparatus. A complete survey is, however, necessary to obtain a detailed account of the contribution in sheath drop with varying magnetic field. The electric field appearing in the equations is given by  $E'_x = E_x - v_\theta B$  where  $E_x$  is the measured quantity. The effect of rotation can reduce  $-j_\theta/j_x$  but it appears unlikely that it would be a strong effect, as  $v_\theta$  the average plasma rotational velocity will be low compared to  $-j_\theta/n_e e$ .

Investigators studying similar devices, although operating at conditions differing from the present case, have found  $E$  versus  $B$  curves in which  $E$  varies first as  $B^2$  then as  $B$  as the  $B$  field is increased. Some have explained this effect on the basis of turbulent Bohm diffusion (refs. 4, 5, 6). However, a recent publication (ref. 12) notes that the inclusion of ion motion in the theory reduces the effect of turbulence. Others have explained the effect on the basis of  $n_e/B$  becoming constant at high  $B$  (ref. 7). These theories will be discussed further in reference 13. It appears that under the operating conditions reported in this thesis, the simple theory involving the variation of  $W$  with  $B$  is adequate to explain the experimental results. Additional measurements as suggested in the section entitled "Operation of Discharge and Measurements" are necessary before this theory can be substantiated.

#### REFERENCES

1. Hess, R. V.: Experiments and Theory for Continuous Steady Acceleration of Low Density Plasma. Vol. I of Proc. XI International Astronautical Congress, August 1960, C.W.P. Reuterswärd, ed., Springer Verlag (Vienna), 1961, pp. 404-411.
2. Hess, R. V. and others: Oral presentation, Third NASA Inter-Center Meeting on Magnetoplasmodynamics, April 1962.
3. Rigby, R. H.: Some Physical Properties of an Axial Electric Arc in a Radial Magnetic Field. M. A. Thesis, The College of William and Mary, Va., August 1962.
4. James, G. S., Dotson, J., and Wilson, T.: Electrostatic Acceleration of Neutral Plasmas. Momentum Transfer Through Magnetic Fields. Avco-Everett Res. Lab. AMP 88, September 1962.
5. Salz, F., Meyerand, R. G., Jr., and Lary, E. C.: Ion Acceleration in a Gyro-Dominated Neutral Plasma Experiment. Bulletin American Phys. Soc. Ser. II, Vol. 7, No. 7, p. 441, August 1962.
6. Yoshikawa, S., and Rose, D. J.: Anomalous Diffusion of a Plasma Across a Magnetic Field, The Physics of Fluids, Vol. 5, No. 10, pp. 1272-1277, October 1962.
7. Chubb, D. L.: Hall Current Ion Accelerator. Fourth Symposium on the Engineering Aspects of Magnetohydrodynamics, April 1963 (Oral Presentation).

8. Camm, G. L., Ziermer, R. W., and Marlotte, G. L.: The Hall Current Plasma Accelerator. Electro-Optics, Inc., Presented at the ABE Electric Propulsion Conference, Colorado Springs, Colorado, March 1963.
9. Hess, R. V., Rigby, R. N., and Weinstein, R. H.: Observation of Hall Currents for A D-C Axial-Arc Discharge in a Radial Magnetic Field. Bulletin American Phys. Soc., Serv. II, Vol. 8, No. 2, p. 168, Feb. 1963.
10. Hess, R. V., Burlock, J., Sevier, J. R., and Brockman, P.: Theory and Experiments for the Role of Space Charge in Plasma Acceleration. Symposium on Electromagnetics and Fluid Dynamics of a Gaseous Plasma. April 1961. Vol. XI of Microwave Res. Inst. Symposia Ser., Polytechnic Press of Polytechnic Inst. of Brooklyn, pp. 269-305, 1962.
11. Bohm, D., Burhop, E. H. S., and Massey, H. S. W.: The Use of Probes for Plasma Exploration in Strong Magnetic Fields. Characteristics of Electrical Discharges in Magnetic Fields. Edited by A. Guthrie and R. K. Wakerling, McGraw-Hill, 1949.
12. Kadomtsev, B. B.: Turbulent Plasma in a Strong Magnetic Field. Journal of Nuclear Energy, Part C (Plasma Physics), Vol. 5, pp. 31-36, 1963.
13. Brockman, P., Hess, R. V., and Weinstein, R. H.: Measurements and Theoretical Interpretation of Hall Currents for Steady Axial Discharges in Radial Magnetic Fields, to be presented at the Fifth Biannual Gas Dynamics Symposium, August 1963.

## VITA

Born in Boston, Massachusetts, November 28, 1937. Graduated Newton High School, Newton, Massachusetts, June 1955. Bachelor of Science degree at University of Massachusetts, June 1959. In September 1960, the author entered the College of William and Mary as a Master of Arts candidate in Physics. The author has been employed by the National Aeronautics and Space Administration, Langley Research Center, Hampton, Virginia, from July 1959 to present as a research engineer.